Segmentation of low-grade glioma using MRI images of the brain

Overview

1. Problem Statement
2. Data Overview
3. Methodology Selection
4. Training Process
5. Results Overview
6. Comparison with Existing Solutions

Problem Definition & Overview

Segmentation of low-grade glioma using MRI images of the brain

This project proposes to segment low-grade gliomas based on a dataset from the cancer imaging archive The Cancer Genome Atlas (TCIA). The dataset contains MR images of the brain along with manually generated FLAIR anomaly segmentation masks. Tumor genomic clusters and patient data are presented in the data.csv file.

The data is at the link. Based on this dataset, a kaggle competition was created, in which you are invited to participate.

The goal of the project is to build a segmentation model to solve the problem of segmenting a tumor using an anomaly mask. Compare the obtained metrics with existing solutions and present the best model and your results.

Dataset Structure

The structure of the dataset is a bit unusual since it contains the same data two times: the folders *kaggle_3m* contain exactly the same data.

```
.
+-- kaggle_3m
|    +-- TCGA_CS_4941_19960909
|    +-- TCGA_CS_4942_19970222
|    +-- ...
|    +-- ...
|    +-- ...
|    +-- TCGA_HT_A61A_20000127
+-- lgg-mri-segmentation
     +-- kaggle_3m
```

Dataset Description

From *README.md* of the dataset:

All images are provided in *.tif* format with 3 channels per image. For 101 cases, 3 sequences are available, i.e. pre-contrast, FLAIR, post-contrast (in this order of channels).

For 9 cases, post-contrast sequence is missing and for 6 cases, pre-contrast sequence is missing. Missing sequences are replaced with FLAIR sequence to make all images 3-channel. Masks are binary, 1-channel images. They segment FLAIR abnormality present in the FLAIR sequence (available for all cases).

The dataset is organized into 110 folders named after case ID that contains information about source institution. Each folder contains MR images with the following naming convention:

TCGA_<institution-code>_<patient-id>_<slice-number>.tif

Corresponding masks have a *_mask* suffix.

Examples from Dataset

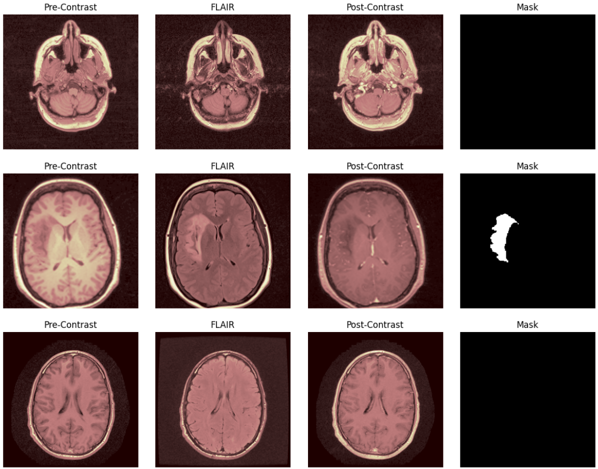

Figure: 3 channels of input image and target binary mask

File with Tabular Data

The provided dataset includes information related to each patient. However, it lacks specific details for individual images. This limitation makes the dataset unsuitable for our analysis.

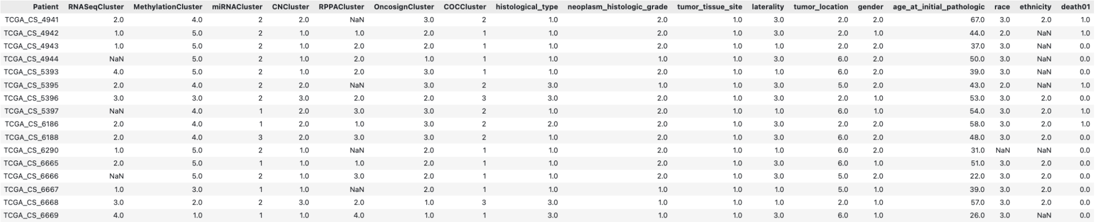

Patient	RNASeqCluster	MethylationCluster	miRNACluster	CNCluster	RPPACluster	OncosignCluster	COCCluster	histological_type	neoplasm_histologic_grade	tumor_tissue_site	laterality	tumor_location	gender	age_at_initial_pathologic	race	ethnicity	death01
TCGA_CS_4941	2.0	4.0	2	2.0	NaN	3.0	2	1.0	2.0	1.0	3.0	2.0	2.0	67.0	3.0	2.0	1.0
TCGA_CS_4942	1.0	5.0	2	1.0	1.0	2.0	1	1.0	2.0	1.0	3.0	2.0	1.0	44.0	2.0	NaN	1.0
TCGA_CS_4943	1.0	5.0	2	1.0	2.0	2.0	1	1.0	2.0	1.0	1.0	2.0	2.0	37.0	3.0	NaN	0.0
TCGA_CS_4944	NaN	5.0	2	1.0	2.0	1.0	1	1.0	1.0	1.0	3.0	6.0	2.0	50.0	3.0	NaN	0.0
TCGA_CS_5393	4.0	5.0	2	1.0	2.0	3.0	1	1.0	2.0	1.0	1.0	6.0	2.0	39.0	3.0	NaN	0.0
TCGA_CS_5395	2.0	4.0	2	2.0	NaN	3.0	2	3.0	1.0	1.0	3.0	5.0	2.0	43.0	2.0	NaN	1.0
TCGA_CS_5396	3.0	3.0	2	3.0	2.0	2.0	3	3.0	2.0	1.0	3.0	2.0	1.0	53.0	3.0	2.0	0.0
TCGA_CS_5397	NaN	4.0	1	2.0	3.0	3.0	2	1.0	2.0	1.0	1.0	6.0	1.0	54.0	3.0	2.0	1.0
TCGA_CS_6186	2.0	4.0	1	2.0	1.0	3.0	2	2.0	2.0	1.0	3.0	2.0	2.0	58.0	3.0	2.0	1.0
TCGA_CS_6188	2.0	4.0	3	2.0	3.0	3.0	2	1.0	2.0	1.0	3.0	6.0	2.0	48.0	3.0	2.0	0.0
TCGA_CS_6290	1.0	5.0	2	1.0	NaN	2.0	1	1.0	2.0	1.0	1.0	6.0	2.0	31.0	NaN	NaN	0.0
TCGA_CS_6665	2.0	5.0	1	1.0	1.0	2.0	1	1.0	2.0	1.0	3.0	6.0	1.0	51.0	3.0	2.0	0.0
TCGA_CS_6666	NaN	5.0	2	1.0	3.0	2.0	1	1.0	2.0	1.0	3.0	5.0	2.0	22.0	3.0	2.0	0.0
TCGA_CS_6667	1.0	3.0	1	1.0	NaN	2.0	1	1.0	1.0	1.0	1.0	5.0	1.0	39.0	3.0	2.0	0.0
TCGA_CS_6668	3.0	2.0	2	3.0	2.0	1.0	3	3.0	1.0	1.0	1.0	2.0	1.0	57.0	3.0	2.0	0.0
TCGA_CS_6669	4.0	1.0	1	1.0	4.0	1.0	1	3.0	1.0	1.0	3.0	6.0	1.0	26.0	3.0	NaN	0.0

Figure: *data.csv*

Base U-Net

The core component of the binary segmentation model is an U-Net, which is responsible for identifying the location of the tumor within the image (if there is a tumor). The model has 31 million parameters:

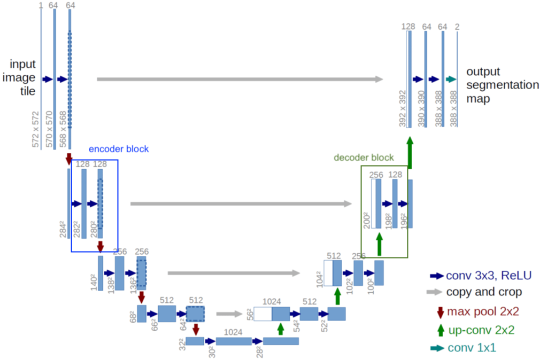

Figure: U-Net

Convolution with Multiple Channels

In the U-Net architecture convolutional layers are utilized, and it is important to monitor the number of channels in both the input and output. In the encoding phase, the number of channels increases, stays the same at the bottleneck, and then decreases during the decoding phase. Below are examples of convolutions with multiple channels for reference:

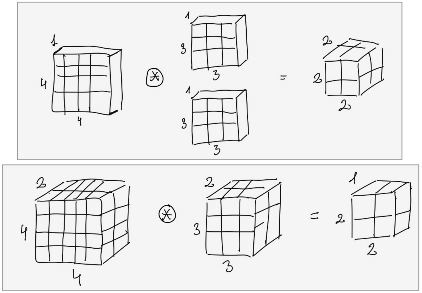

Figure: Examples of convolution

ResNet

Preceding this, the auxiliary component of the model is a ResNet, which serves to identify the presence of a tumor in the image:

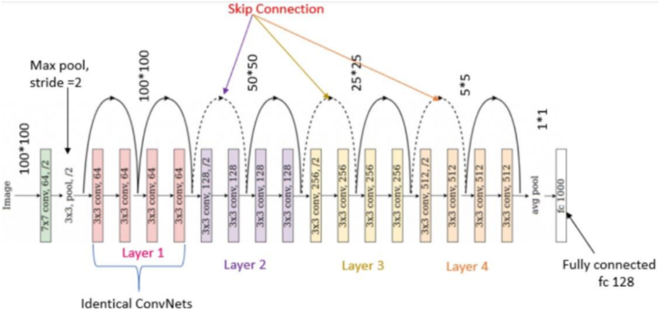

Figure: ResNet18

Alternative U-Net Architecture

For the core component, we will additionally implement a simplified version of the U-Net. This model has 1,8 million parameters:

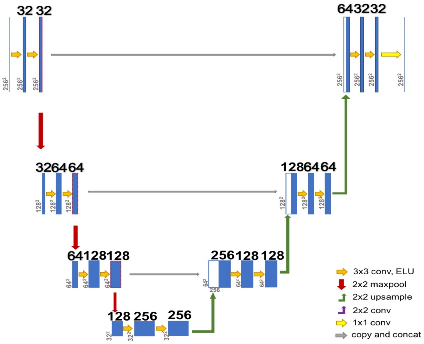

Figure: U-Net mini

Loss Function: BCEWithLogitsLoss

BCEWithLogistLoss is a loss function that combines the sigmoid activation function and the Binary Cross-Entropy (BCE) loss in a numerically stable way:

$$BCE(y,p) = -\left(y\log(p) + (1-y)\log(1-p)\right)$$

$$BCEWithLogistLoss(y,z) = -[y\log(\sigma(z)) + (1-y)\log(1-\sigma(z))]$$

if we expand using $\sigma(z) = \frac{1}{1+e^{-z}}$:

$$BCEWithLogistLoss(y,z) = max(z,0) - zy + log(1+e^{-|z|})$$

Notice that:

In our case there are significantly more background pixels than glioma pixels. Therefore, we need to assign a proportionally higher weight to the positive glioma errors: for this we use $\mathtt{pos\_weight}$ argument. We apply the same principle in ResNet, but the weighting is adjusted according to the proportion of input images containing gliomas.

Loss Function: Numerical Stability

BCEWithLogitsLoss is numerically stable, let's look at extreme values:

- For large z (e.g., $z = 100$): $\sigma(z) \approx 1, \quad \text{so} \quad \log(1 - \sigma(z)) \approx \log(0)$ which is undefined.
  BCEWithLogitsLoss avoids computing this directly.
- For small z (e.g., $z = -100$): $\sigma(z) \approx 0, \quad \text{so} \quad \log(\sigma(z)) \approx \log(0)$ which is undefined.
  Again, BCEWithLogitsLoss avoids this direct computation.

Training of ResNet

The model was saved on epoch 28:

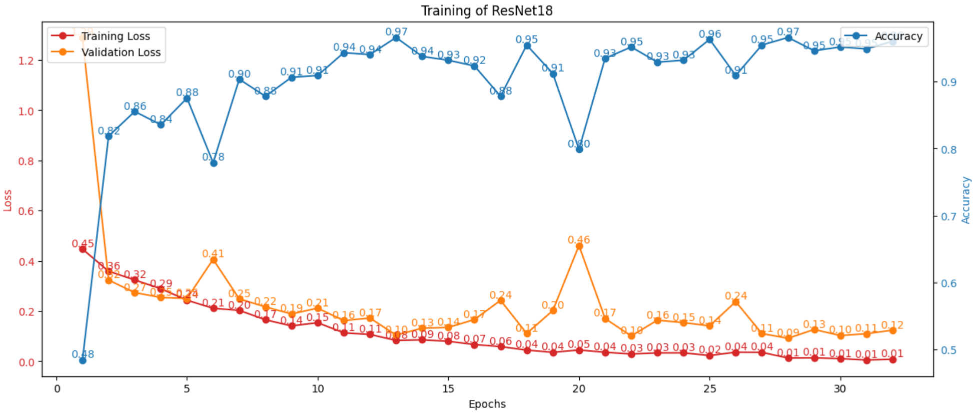

Figure: Training process of ResNet18

Training of U-Net

The model was saved on epoch 30:

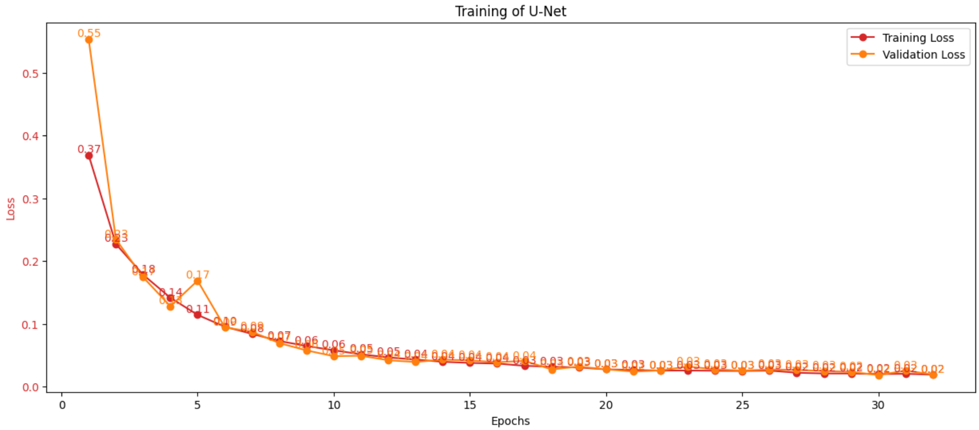

Figure: Training process of U-Net

Training of U-Net Mini

The model was saved on epoch 27:

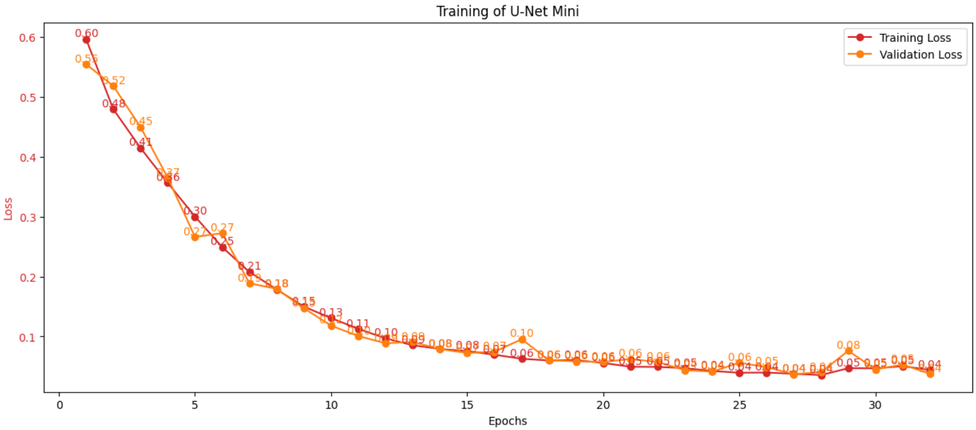

Figure: Training process of U-Net Mini

Test of ResNet

Class	Precision	Recall	F1-Score	Support
No Glioma	0.98	1.00	0.99	268
Glioma	0.99	0.96	0.98	125
Accuracy			0.98	393
Macro Avg	0.99	0.98	0.98	393
Weighted Avg	0.98	0.98	0.98	393

Table: Classification Report for ResNet18

Test of U-Net

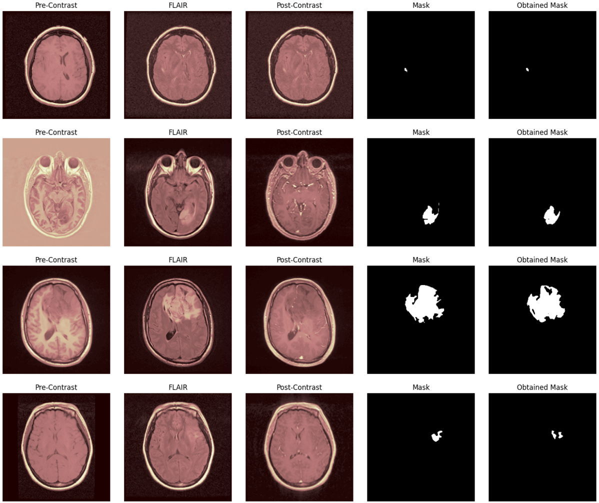
Pre-Contrast
FLAIR
Post-Contrast
Mask
Obtained Mask
Pre-Contrast
FLAIR
Post-Contrast
Mask
Obtained Mask
Pre-Contrast
FLAIR
Post-Contrast
Mask
Obtained Mask
Pre-Contrast
FLAIR
Post-Contrast
Mask
Obtained Mask

Test of U-Net Mini

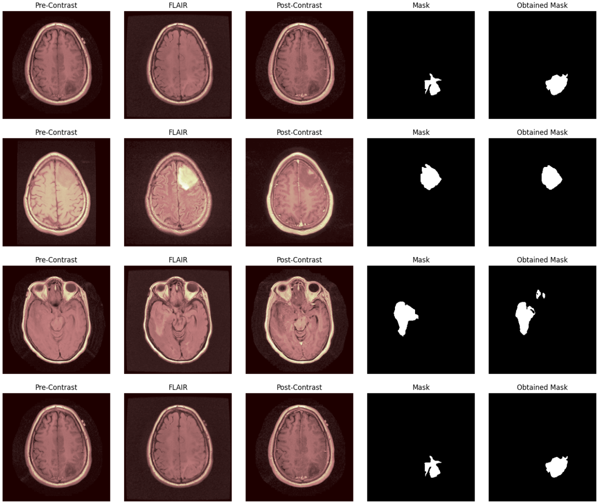

Visual Results Overwiev

Both models demonstrate the ability to accurately locate gliomas. However, the U-Net architecture performs better in precisely segmenting the tumor borders, while the U-Net Mini has difficulty with this task. In contrast, U-Net Mini has 15 times fewer parameters, allowing for significantly faster training times.

Additionally, we achieved a 98% accuracy with the ResNet model, so when combined, we should obtain a reliable segmentation model.

Dice Loss

For the final evaluation, we will use the Dice loss function, as it highlights the overlap between the target and the output:

$$\text{IoU} = \frac{|A \cap B|}{|A \cup B|}, \quad \text{Dice} = \frac{2|A \cap B|}{|A| + |B|}, \quad \text{Dice Loss} = 1 - \text{Dice}$$

Notice that:

We add a small constant value to the numerator and denominator of Dice loss to ensure that the loss function remains valid in situations where there is no overlap.

Evaluation of Models

	All Images	**Only with Glioma**
ResNet18 + U-Net	93.12%	79.15%
ResNet18 + U-Net Mini	89.85%	68.90%

Table: Dice Coeff.

Comparison with Other Competitors

- The most voted answer on kaggle.com achieved a 92.0% IoU with the "U-Net with ResNext50 backbone," resulting in:

  $$\text{Dice} = \frac{2 \cdot \text{IoU}}{1 + \text{IoU}} = 96\%$$

  This result is superior to ours.
- The second most voted answer obtained an 89.6% Dice coefficient using a U-Net. Our result surpasses this.

Overall, our model is competitive in this context.

Other Possible Approaches

In the review article ”U-Net and Its Variants for Medical Image Segmentation” by N. Siddique et al. (IEEE Access, vol. 9, pp. 82031-82057, 2021, doi: 10.1109), numerous examples of tumor segmentation in the brain are presented. Here are some potential architectures for future consideration:

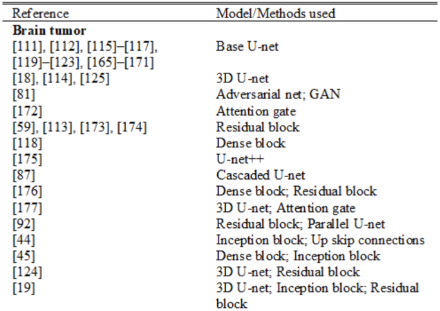

Reference	Model/Methods used
Brain tumor	
[111], [112], [115]–[117], [119]–[123], [165]–[171]	Base U-net
[18], [114], [125]	3D U-net
[81]	Adversarial net; GAN
[172]	Attention gate
[59], [113], [173], [174]	Residual block
[118]	Dense block
[175]	U-net++
[87]	Cascaded U-net
[176]	Dense block; Residual block
[177]	3D U-net; Attention gate
[92]	Residual block; Parallel U-net
[44]	Inception block; Up skip connections
[45]	Dense block; Inception block
[124]	3D U-net; Residual block
[19]	3D U-net; Inception block; Residual block

Figure: Possible Implementations

The End